The Effects of Rotation-Induced Mixing on the Properties of Secondary-Clump Stars

Lorenzo Martinelli (master's student)

University of Bologna

E-mail: lorenzo.martinelli3@studio.unibo.it

Supervisor: Andrea Miglio

Lorenzo Martinelli, Andrea Miglio[1], Patrick Eggenberger[2], Gaël Buldgen[2,3]

1. Dipartimento di Fisica e Astronomia "Augusto Righi", Università di Bologna, Bologna, Italy

2. Département d'Astronomie, Université de Genève, Chemin Pegasi 51, CH-1290 Versoix, Switzerland

3. STAR Institute, Université de Liège, Liège, Belgium

Abstract

Stellar age determinations are affected by uncertainties due to internal mixing processes. We focus on the efficiency of mixing near convective cores, especially induced by rotation, during core hydrogen-burning. Our innovative approach examines the impact of such mixing on the luminosity distribution and core properties of core helium-burning stars. By creating synthetic stellar populations with varying ages and rotation-induced mixing, we obtain extended red clumps in single-age synthetic clusters. These features offer insights into the possible origin of extended red clumps and turn-offs, to the efficiency of rotational mixing of chemicals and to the impact on age determinations. An initial assessment comparing the results with observations appears to support the plausibility of this scenario to some extent.

Methods

We computed a grid of non-rotating MESA (Paxton et al. 2019) models with additional mixing calibrated during the MS on some reference rotating GENEC (Eggenberger et al. 2008) models in order to mimic rotational mixing from an advecto-diffusive treatment.

The range of masses and rotations covered by the grid is $1.7 - 3.0\ M_\odot$ ($\Delta M = 0.025$) and $0.0, 0.3, 0.5, 0.6, 0.7, 0.8, 0.9, 0.95\ \Omega/\Omega_c$.

The calibration is based on 5 parameters of the star that are sensitive to rotational mixing and it consists in the minimization of the RMSE of these parameters with respect to reference values taken from GENEC models (Georgy et al. 2013 b).

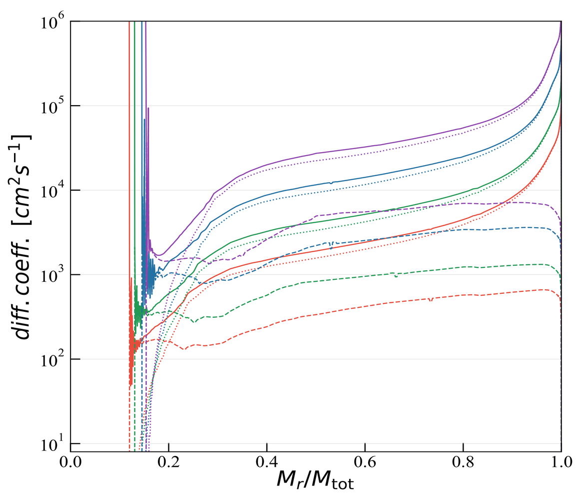

Fig.1: Profiles of the diffusion coefficients in the reference GENEC models. D_{mix} (solid), D_{eff} (dashed) and D_{shear} (dotted) of a 1.7 M⊙ (red), 2.0 M⊙ (green), 2.5 M⊙ (blue), 3.0 M⊙ (violet) models at roughly the middle of the MS phase ($X_{H,c} = 0.03$) for $\Omega_{ini}/\Omega_{crit}$=0.5.

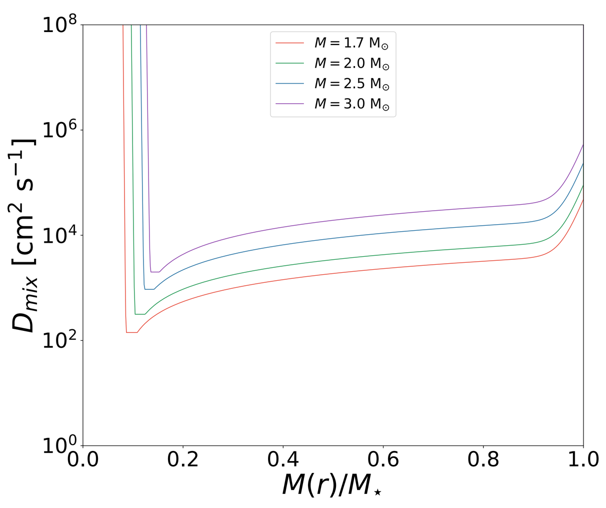

Fig.2: Profiles of the diffusion coefficient D_{mix} (solid) in the calibrated MESA models, of a 1.7 M⊙ (red), 2.0 M⊙ (green), 2.5 M⊙ (blue), 3.0 M⊙ (violet) models for $\Omega_{ini}/\Omega_{crit}$=0.5.

The calibrated models can reproduce with fairly good accuracy all the features caused by rotational mixing of chemicals in GENEC, with all the benefits of using MESA (computation of He flash, computing large grids, interface with GYRE).

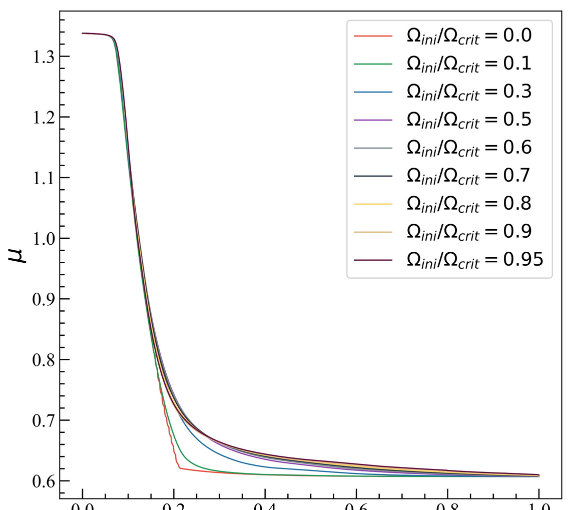

Fig.3: Mean molecular weight profiles at TAMS for 2.5 M⊙ GENEC reference models for 0.0, 0.1, 0.3, 0.5, 0.6, 0.7, 0.8, 0.9, 0.95 $\Omega_{ini}/\Omega_{crit}$.

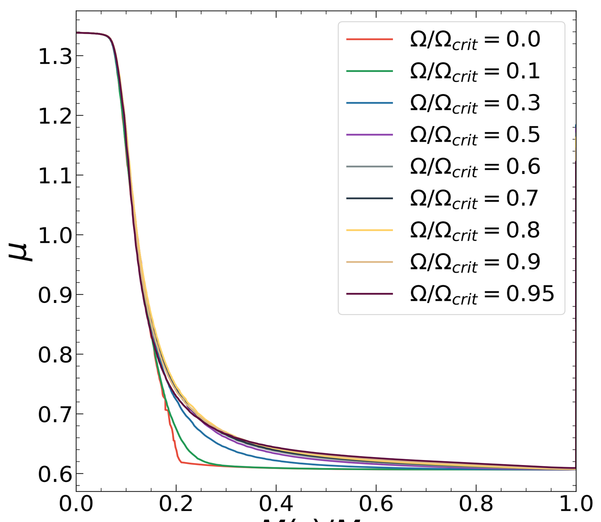

Fig.4: Mean molecular weight profiles at TAMS for 2.5 M⊙ MESA calibrated models for 0.0, 0.1, 0.3, 0.5, 0.6, 0.7, 0.8, 0.9, 0.95 Ωini/Ωcrit.

Being a diffusive process acting both near the core and in the whole envelope, rotational mixing is expected to:

- enlarge the mass of the convective core by bringing fresh hydrogen in the H-burning region, resulting in a bigger He core and age at the TAMS
- create an extended μ gradient in the envelope.

Results

During the Quiescent Core He Burning (QCHeB) phase, the details of the μ profile introduced by rotational mixing are obliterated by the deep penetration of the convective envelope during the red giant phase.

Nevertheless, the impact on the size of the He core and on the μ in the envelope are enough to produce significant effects on L, T_{eff} and R distributions.

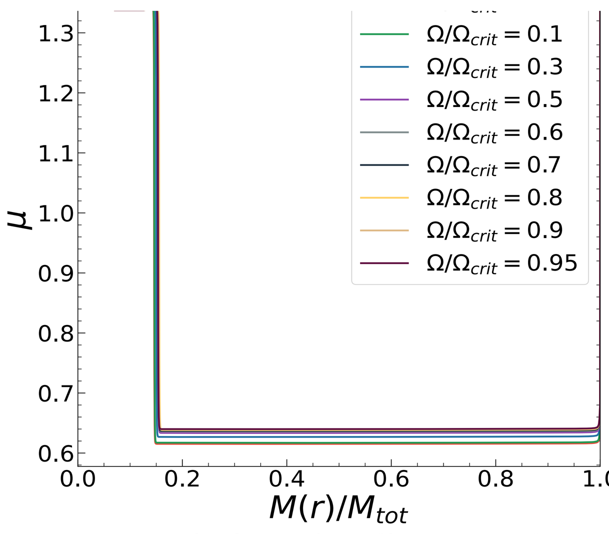

Fig.4: Mean molecular weight profiles at QCHeB for 2.5 M⊙ MESA calibrated models for 0.0, 0.1, 0.3, 0.5, 0.6, 0.7, 0.8, 0.9, 0.95 Ωini/Ωcrit.

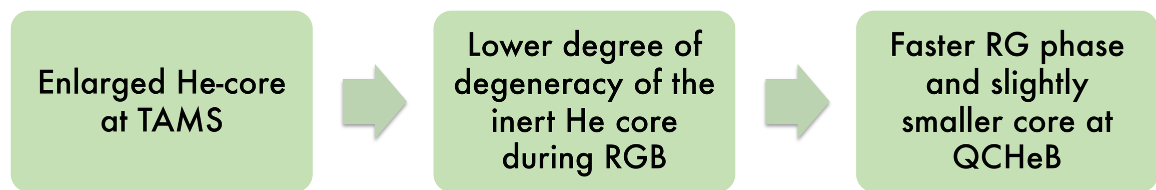

(true on the low-mass side of the M_{Hef} transition when degeneracy still plays a role)

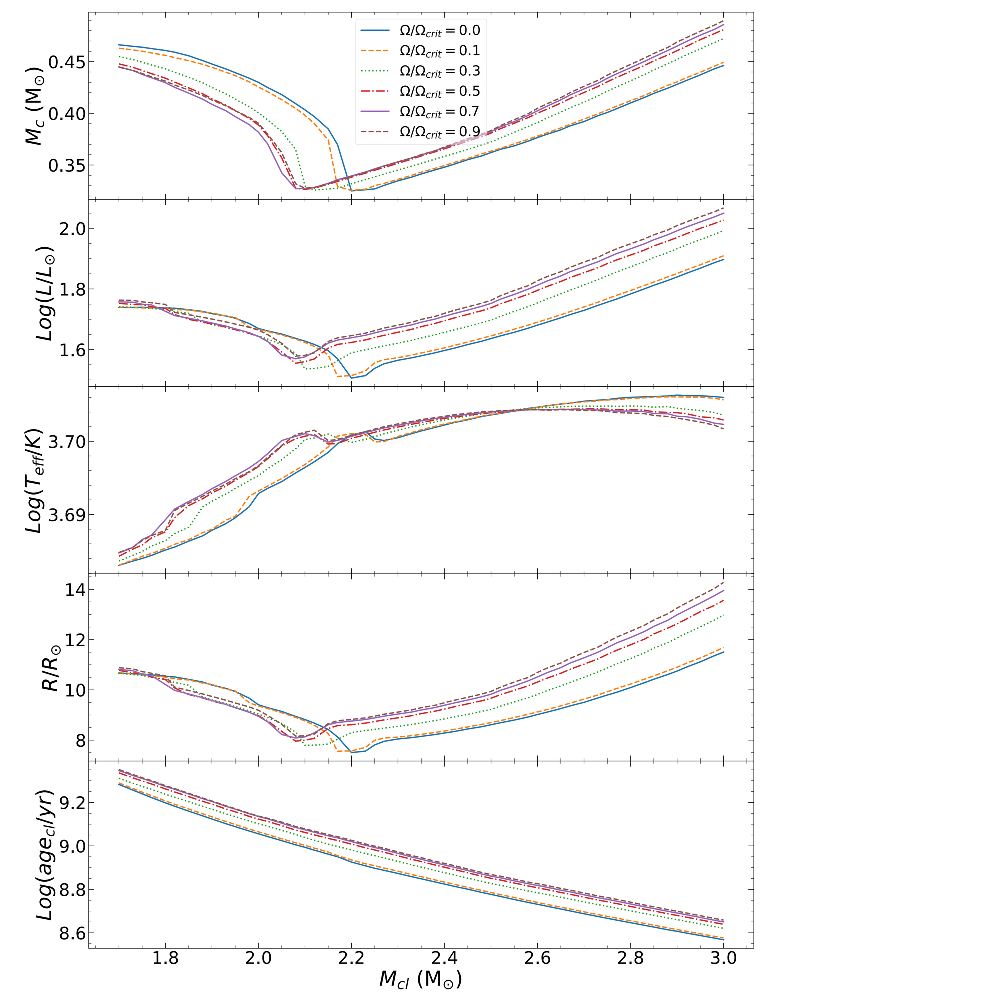

Fig. 5: Mass of the He core M_c, luminosity, effective temperature and radius as a function of the total mass of the star at the clump M_{cl} with different initial values of Ω/Ω_c and overshooting.

Because of the complex interplay between age, L, R, T_{eff} the expected impact on stellar populations is better seen by computing isochrones or synthetic stellar populations.

Synthetic Stellar Populations

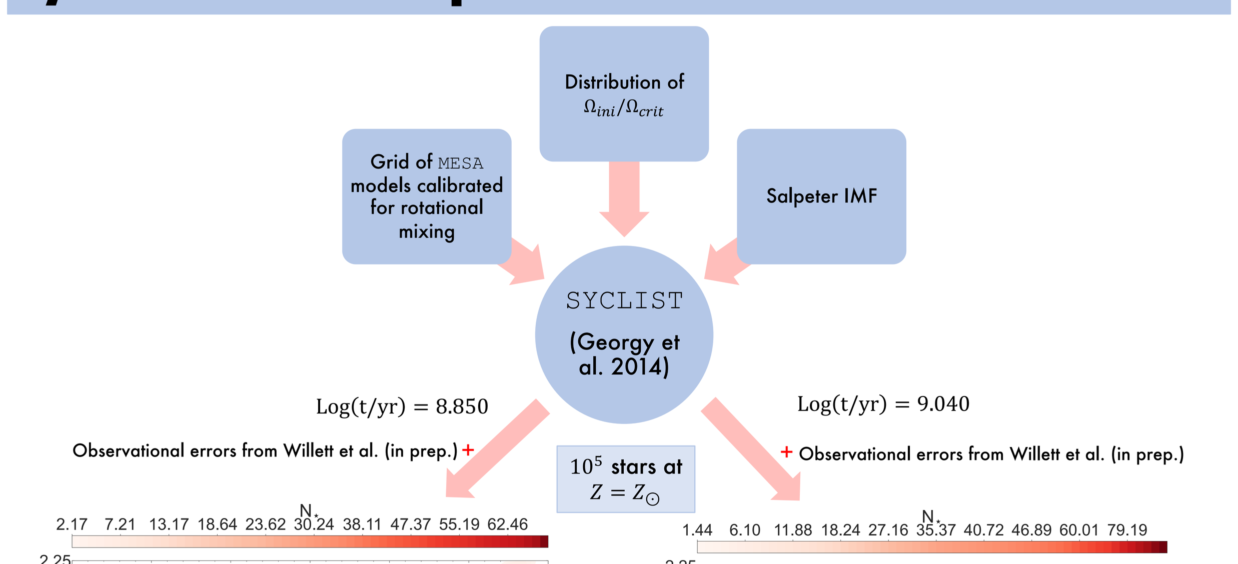

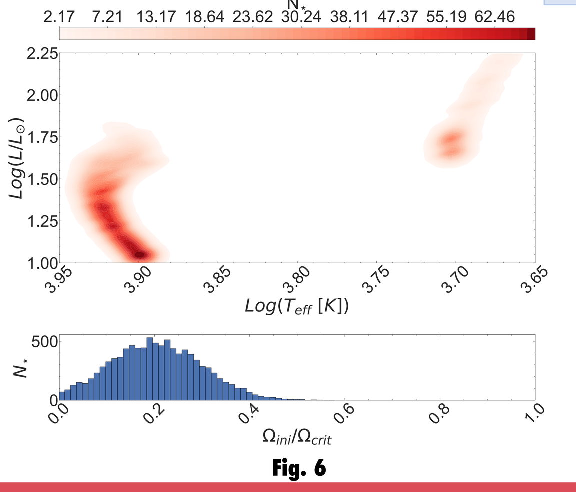

Fig. 6

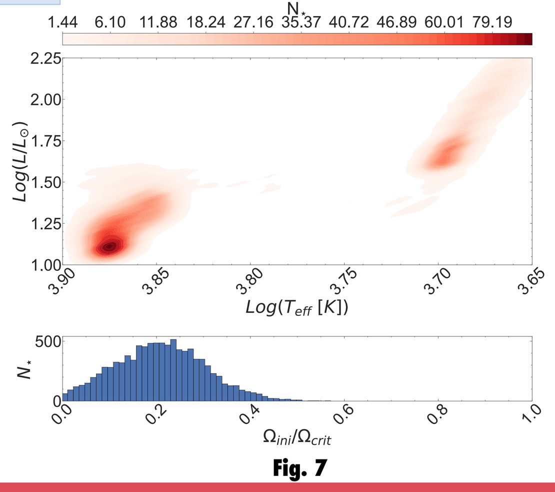

Fig. 7

Extended red clumps

We see that, due to the spread in initial rotation we have the appearance of an extended red clump in the age range $8.700 < Log(t/yr) < 9.200$.

Within this range the extended clumps seems to invert their properties at a specific age t_{inv} with:

$$8.850 < Log(t_{inv}/yr) < 9.040\,.$$

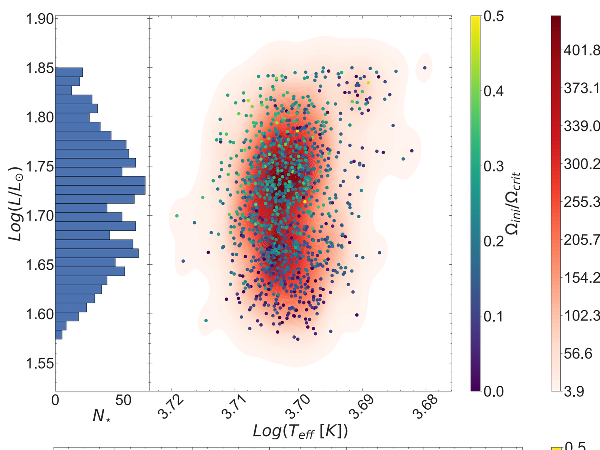

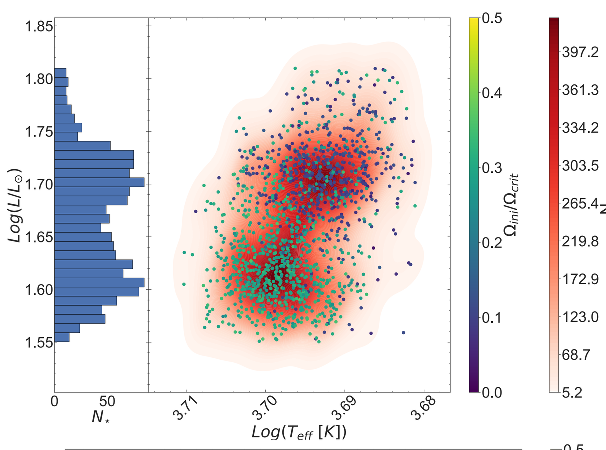

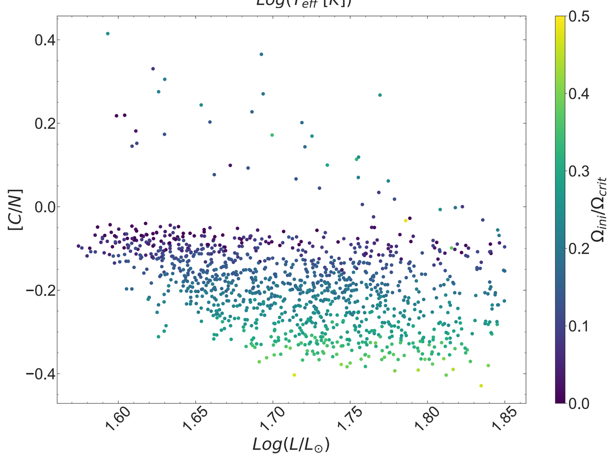

Fig. 8: Focus on the properties of the extended red clump in Fig. 6.

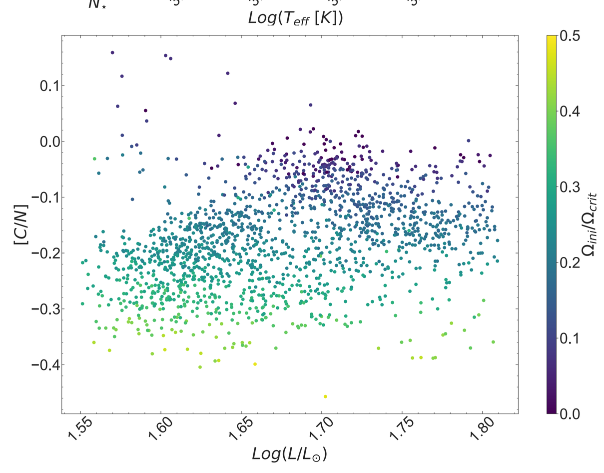

Fig. 9: Focus on the properties of the extended red clump in Fig. 7.

A spread in initial rotation could be one of the origins of the observed extended red clumps, e.g. in NGC 419 (Girardi et al. 2009 and Dresbach et al. 2023). If this is the case we should be able to observe a spread in [C/N] which reflects the Ω_{ini}/Ω_c distribution.

Comparison with observations

We compared the properties of red clump stars with $Z \approx Z_\odot$ in our single-age synthetic clusters, with Ω_{ini}/Ω_c distributions from Royer et al. 2007, with red clump stars from the Galactic field (Willett et al. in prep.), NGC 6811(Sandquist et al. 2016) and NGC 6866 (Brogaard et al. 2023).

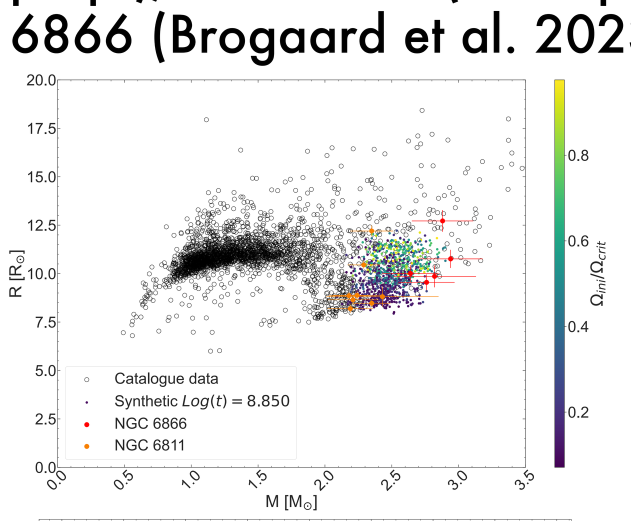

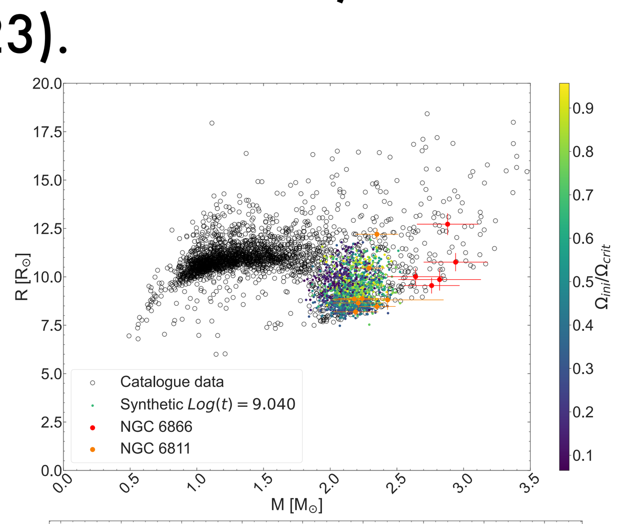

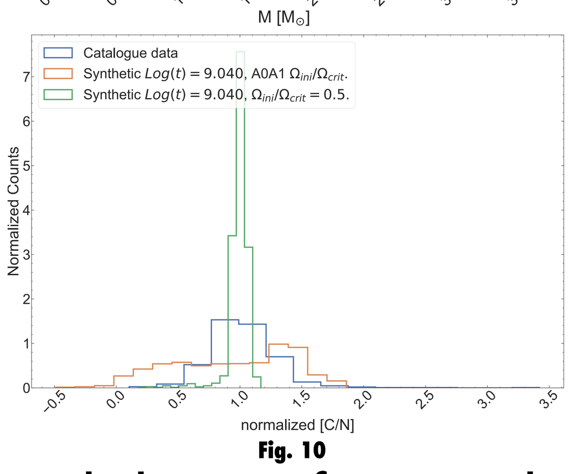

Fig. 10

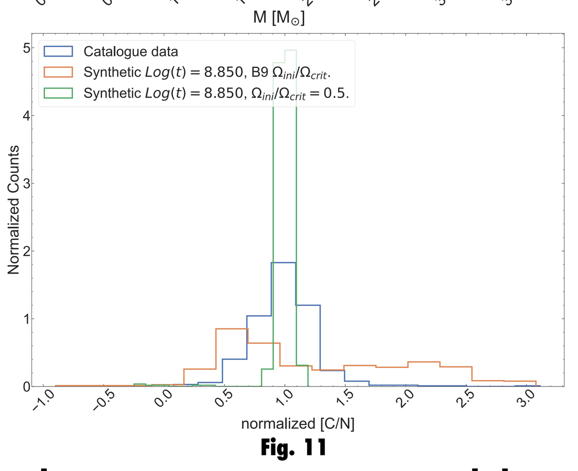

Fig. 11

Red clumps of our synthetic clusters are compatible with having both RC1 and RC2 stars and have a [C/N] spread compatible with data (not the case for a single value of Ω_{ini}/Ω_c .

ASTEROCHRONOMETRY

erc European Research Council

References:

1. Paxton, et al., 2019, ApJS, 243, 1
2. Eggenberger et al. 2008, Ap&SS, 316, 1-4
3. Georgy et al. 2013 b, A&A, 553, A24
4. Georgy et al. 2014, A&A, 566, A21
5. Willett et al. (in prep.)
6. Girardi et al. 2009, MNRAS, 349, 1
7. Dresbach et al. 2023, arXiv e-prints, art. arXiv:2310.01499
8. Sandquist et al. 2016, ApJ, 831, 1
9. Brogaard et al. 2023, arXiv e-prints, art. arXiv:2308.12731
10. Royer et al. 2007, A&A, 463, 2